Hindawi
Journal of Applied Mathematics
Volume 2023, Article ID 7193935, 9 pages
https://doi.org/10.1155/2023/7193935

Research Article

3D Modeling of Mine Protection Complex Steel Structure Based on BIM Technology

Fenhong Li[1], **Zaisheng Wang**[2], **Chongan Pang**[1] and **Haiping Yang**[1]

[1]*College of Architectural Engineering, Zhejiang Tongji Vocational College of Science and Technology, Hangzhou 311231, China*
[2]*General Manager's Office, Zhejiang Zhongnan Construction Group Steel Structure Co., Ltd., Hangzhou 310052, China*

Correspondence should be addressed to Fenhong Li; lifenhong@mjc-edu.cn

Received 19 September 2022; Revised 6 December 2022; Accepted 21 February 2023; Published 6 March 2023

Academic Editor: Waqar A. Khan

The objective of this paper is to study the antidamage ability of beam column joints in complex steel structures under external forces and to improve the safety of such structures. In this study, a three-dimensional model of complex steel structure based on BIM technology is proposed by analyzing and calculating the ultimate strength of complex steel structure for mine protection. The vibration control algorithm of complex steel structure for mine protection is designed, and the boundary elastic constraint conditions are determined. According to the constraint conditions, the vibration characteristics of complex steel structures for mining are analyzed. The experimental results show that the maximum displacement of the design model is reduced by half compared with that before optimization, which can meet the design requirements.

1. Introduction

The safety and durability of mine protection depend on the vibration isolation, vibration reduction, and vibration control capabilities of the damping structure to a certain extent [1]. Generally, the construction unit and technicians select excellent protective materials to improve the function of the complex steel structure for mine protection, so as to ensure that the mine protection can maintain its safety performance in a longer service period. Steel structure is a structure composed of steel materials, which is one of the main types of mine protective structures. The steel structure is mainly composed of beam steel, steel column, steel truss, and other components made of section steel and steel plate and undergoes rust removal and rust prevention processes such as silane, pure manganese phosphating, cleaning and drying, and galvanizing [2]. When the proportion of steel increases in all kinds of construction steel, the application of more complex steel structures in mine protection engineering has become an inevitable trend, and 3D modeling has a huge development prospect in steel structures.

Ye et al. proposed a driving force model for fatigue crack growth of CFRP-strengthened steel structures [3]. Through the fatigue tests of various steel members and the corresponding finite element simulation, the crack growth rate and the accuracy of life prediction are tested. The fatigue mechanism of unstressed and prestressed CFRP-strengthened damaged steel structures is analyzed. At the same time, by analyzing the elastic seismic performance and design of LVEM isolation layer of single-layer steel structure and using laminated viscoelastic materials for floor isolation, the seismic requirements of the structure can be reduced [4]. The elastic seismic behavior of single-story steel structure with LVEM isolation layer system is studied. The numerical simulation method and dynamic analysis program of the structural system are established. The validity of the numerical simulation method is verified by shaking table test. On this basis, a 3D modeling method of complex steel structure for mine protection based on BIM technology is

proposed. BIM technology is a building information model technology, integrating various kinds of building engineering information; based on which, a three-dimensional building model can be established. The BIM technology is applied throughout the entire life cycle of the construction project, and the combination of information collection, BIM technology, and traditional work mode does not have the advantages that collaborative management mode has. It changes the defects of traditional extensive construction and realizes the transformation of advanced intensive construction mode. As an innovative method in construction control and visual simulation, it can realize visual effect design, check model renderings, and realize 4D effect model design and monitoring functions. This is also the reason why BIM technology is applied to 3D modeling and analysis of complex steel structures for mine protection in this study.

2. Three-Dimensional Modeling of Complex Steel Structure for Mine Protection Based on BIM Technology

2.1. Design of Vibration Control Algorithm for Mine Protection Complex Steel Structure. When the mine is faced with serious vibration, the mine can consume seismic energy through the parts resisting lateral force. The components resisting lateral force mainly rely on the elasticity and deformation of energy consuming components to absorb huge energy, thus reducing the losses of the mine [5]. Based on BIM technology, the seismic system for protecting complex steel structures in the mine is realized through the isolation layer of the mine. It is necessary for mine designers to reasonably distinguish different parts of the mine steel structure by adding isolation layers in the complex steel structure. According to the seismic energy conduction, the isolation layer of the building is arranged between the upper structure and the lower structure. The principle of this isolation method is that the lower mine protection composite steel structure absorbs most of the vibration energy. After the isolation, the upper structure can reach the elastic state or even be intact in case of vibration.

To seek the safety standard of blasting vibration of steel structure, it is necessary to determine the amplitude of input vibration wave in the critical state when a member of steel structure is about to crack. In the process of actual dynamic finite element analysis of steel structure under vibration wave action, it was found that the failure of masonry structure generally occurred when the first principal stress of structural element reached the failure stress value first and then failed with given structure type and material model [6]. Then, the failure cracking of steel structure was in the instantaneous state when the first principal stress of a structural element reached the value of failure stress. Seeking this critical state requires many cycles of time-consuming calculation, and the critical state sought is not necessarily the true failure critical state [7]. In this work, the following processing methods were adopted to determine the safety standard of blasting vibration. If there is no element failure in the structure when the amplitude of the input blasting seismic wave is equal to v_1 and there is element failure in the structure when the amplitude increases to 1.05 v_1, then the former state is defined as the critical failure state of the structural element, and v_1 is determined as the safety standard value of vibration. The above determination method was used to seek the vibration safety standard of complex steel structure for mine protection based on BIM technology. Firstly, a typical structure and appropriate material constitutive of mine were selected for finite element modeling. The vibration velocity wave of each main frequency band was applied as input load to the base node of the finite element model of masonry structure. Since the frequency band of vibration wave was relatively wide, it was impossible to take all the seismic waves of each main frequency [8]. Take one measured vibration wave in the frequency band [10 Hz, 10 Hz to 50 Hz, 50 Hz to 100 Hz], and set the duration as 0.2 s. The amplitude can be adjusted by the coefficient. By checking the dynamic finite element analysis results and adjusting the vibration amplitude alternately, the safety standard value of blasting vibration is determined.

2.2. Boundary Elastic Constraint Conditions for Vibration Control of Steel Structures. In the research on vibration of complex steel structure for mine protection based on BIM technology, the boundary elastic constraint conditions can be assumed as the constraint of displacement spring; that is, the displacement mode in the displacement direction can be determined by the assumption that there is spring constraint in the displacement direction [9]. When the spring is infinite or when the stiffness of the spring is assumed to be 1e12, the fixed support boundary or the displacement in the direction is completely limited. If the stiffness of the spring is 0e12, it can be assumed that the displacement in the direction is a free boundary [10]. The vibration characteristics of plate structures can be analyzed by arbitrarily changing the boundary conditions of displacement of plate structures, changing the polar coordinates of right angle plates, and marking the movement displacement of circular plates. As shown in Figure 1, the boundary springs (the tangential spring K1, the radial spring K2, the bending spring K3, and the coil spring K4) of the restraint plate and the annular structure are determined. Therefore, the stiffness of the spring can be changed to analyze the vibration characteristics of circular plate and annular structure under different boundary conditions.

On this basis, the boundary elastic constraints are dimensionless and discretized. The results of parametric dimensionless treatment are shown in

$$\beta = \frac{R_i}{R_o} \times \Omega, \tag{1}$$

where β is the geometric coefficient and Ω is the dimensionless frequency coefficient. Based on Equation (1) and the set boundary elastic constraints, the boundary value problem for the free vibration of steel structures with elastic constraints is formed. Through a series of discrete processing, the setting and determination results of boundary elastic constraints for the vibration control of steel structures are obtained.

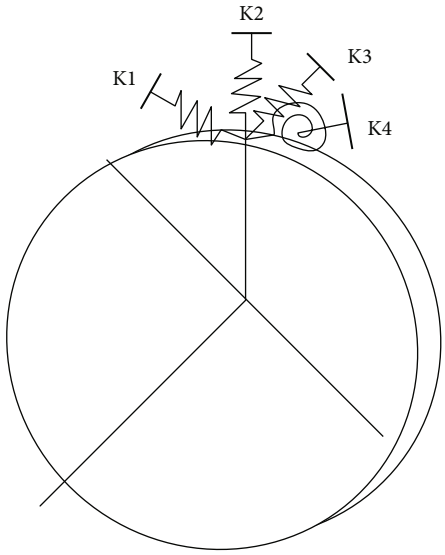

Figure 1: Diagrams of displacement and restraint conditions for mine protection complex steel structures.

After applying BIM technology, the failure strain of unit value has been defined for the mine protection complex steel structure model with N degrees of freedom [11]. In addition, since the tensile strength of masonry materials is low, it is possible to determine whether the unit is damaged by defining the double standard tensile stress value of failure, but it is impossible to determine which critical state is the state of the first unit. When analyzing the structural model, the failure time of the masonry structure to start cracking is considered, and then, the failure elements are deleted for subsequent calculation. Considering the application of BIM technology, the material parameters of the complex steel structure model used for mine protection are shown in Table 1.

2.3. Analysis of Vibration Characteristics of Mine Protection Complex Steel Structure. According to the vibration characteristics of composite structures, this paper selects a reasonable elastic theory and establishes the corresponding energy function considering the boundary elastic constraint [12]. Specifically, considering the vibration characteristics of composite rotating plates and shells and coupled structures, the structural energy function is established based on the first-order shear deformation theory. Based on the functional of structural energy, the governing differential equations and specific expressions of arbitrary boundary conditions are obtained, and the displacement tolerance function of the structure is constructed, which can be applied to arbitrary boundary conditions. By using the modified Fourier series, namely, cosine series and complementary function, the discontinuity of the displacement expression at the boundary can be overcome. The displacement function can be expressed as follows:

$$w(x) = \sum_{m=0}^{\infty} A_m \cos \frac{m\pi x}{\lambda} + p(x), \tag{2}$$

Table 1: Material parameters of complex steel structure model for mine protection.

Category of materials	Masonry	Reinforced concrete
Density (kg/m^3)	1800	2400
Elastic modulus (Pa)	2.99^*10^9	3.0^*10^{10}
Poisson's ratio	0.16	0.2
Yield stress (Pa)	1.29^*10^6	8^*10^6
Hardening modulus (Pa)	6.7^*10^8	5.37^*10^9
Enhancement coefficient	0	0
Failure strain	0.0015	0.00125
Failure stress (Pa)	3^*10^5	2^*10^6

where λ represents the length of the beam in the complex steel structure for mine protection, A_m represents the unknown variable to be solved, and $p(x)$ represents the supplementary function.

For the elastic restraint stiffness of coupling points between adjacent beams, two symbols $k_{i(i-1)}$ and $k_{(i-1)i}$ are named. If they are the rotational elastic restraint stiffness, the two symbols are named $k_{i(i-1)}$ and $k_{(i-1)i}$, and the relationship can be obtained as shown in

$$k_{i(i-1)} = k_{(i-1)i}. \tag{3}$$

The displacement function of generation is constructed, and the Ritz method of displacement function unknown Fourier coefficient of variation is used in the operation. The system of linear equations is obtained by solving the eigenvalue and characteristic vector, and then, the structure of the natural frequencies and corresponding modal vibration mode can be obtained.

2.4. Vibration Response of Complex Steel Structure for Mine Protection by Using BIM Technology. The BIM technique is used to solve the dynamic response of each layer of a multi-degree-of-freedom elastic system under the action of vertical blasting seismic waves. The emergence of BIM technology provides new technical support for mine protection, making the mine protection construction more coordinated and elevating the information level. The application of BIM technology optimizes the mechanical properties and structural safety of mine protection engineering. By discretizing the steel structure system, the dynamic balance formula of the structure system under vibration can be obtained, which is described as follows:

$$M_{I_n}(t) = M_{\ddot{X}} + C_{\dot{X}} + K_X, \tag{4}$$

where $M_{I_n}(t)$ represents the mass of complex steel structure system for mine protection, $C_{\dot{X}}$ represents damping [13], K_X represents stiffness matrix, $\ddot{X}$ represents the acceleration of the structural system relative to the ground, $\dot{X}$ represents the velocity of the system, and X represents the displacement vector. Then, the instantaneous process of the structural system is

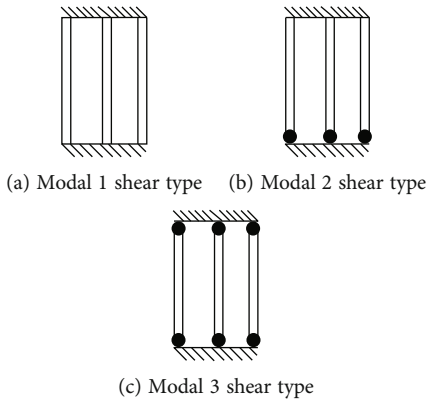

(a) Modal 1 shear type (b) Modal 2 shear type

(c) Modal 3 shear type

Figure 2: Yield mode of shear bracket.

calculated, and the initial conditions are given, so there is

$$\begin{aligned} X(0) &= X_0, \\ \dot{X}(0) &= \dot{X}_0, \end{aligned} \tag{5}$$

where X_0 and $\dot{X}_0$ represent constant vectors, and the displacement of the system at the initial moment is represented by X_0. Given the initial conditions of acceleration and displacement at time t_0, parameters such as acceleration and displacement at time t_1 can be obtained by using the direct integral rule in time domain. According to the above calculation method, the parameter values of $\ddot{X}_t$, $\dot{X}_t$, and X_t at time t can be obtained, and the parameter values at other times can be deduced. Due to the different intensity and frequency of vibration wave at different times, the vibration parameters of complex steel structure for mine protection also vary. The real-time solution results of response parameters obtained are the vibration response of the steel structure.

3. Establishment of Complex Steel Structure Model for Mine Protection

3.1. Limit Strength Analysis of Complex Steel Structures for Mine Protection. In order to facilitate modeling, the bolts in the bracket are all welded to achieve finite element simulation. Specify the I-type interface of shell and solid coupling process, and adjust the degree of freedom between solid units and shell units. Normal direction and tangent direction are set to hard contact and coulomb friction, respectively. Apply 0.2 yield axial pressure on the top of the column, and turn on the large deformation switch in the software to achieve the second-order effect.

In order to verify the ultimate strength of the complex steel structure for mine protection based on BIM technology, it is necessary to load the failure model. During the loading process, the horizontal load is applied according to the position of the inverted triangle, and the multipoint displacement control method is used.

The failure criteria can be divided into three points: (1) the limit stress of the support is close to that of the steel material. (2) The surface stress of the support is close to that of the yielding stress and the plastic hinge appears. (3) The limit stress of any member is close to that of the yielding stress.

In order to verify the ultimate strength of the specimen under different influence conditions, the change of the ultimate strength of the support under different conditions shall be verified, respectively:

(1) Changes in the ultimate strength of pipeline support under different initial defects: usually, not all pipeline supports in mine protection are made of brand-new support material, and they cannot avoid the damage in the process of material transportation. In addition to this transport damage, the impact point or geometrical deviation of the bracket during forging and installation results in different degrees of damage defects within the material will affect the ultimate strength of the bracket to varying degrees. In order to verify the effect of initial imperfections on the ultimate strength of bracket, the initial imperfections are applied to the experimental specimens to reveal the change of the ultimate strength. In order to simplify the calculation process, the uniform imperfection mode is selected to analyze the influence of initial imperfection on the ultimate strength of specimen. To realize the interaction of pile diagrams, the flexural modes of the first and second stages are selected and the strength is calculated, and 1/300 of the bracket is set as the maximum geometric deviation. The yield mode case is shown in Figure 2. The test shall be conducted according to American Society for Testing and Materials (ASTM) standards

(2) Variation of ultimate strength of pipeline support under different transverse deformation conditions: in the artificial construction of pipeline support, errors will occur, which will cause different degrees of deformation of the erected support. Three different ranges (1 m, 2 m, and 3 m) of transverse deformation are given, and the variation of ultimate strength of finite element model of pipeline support is analyzed

3.2. Ultimate Strength Calculation. After the construction of model, the simulation results of pipeline support under various working conditions and loading conditions are obtained. The limit strength of pipeline support change is calculated.

Assume that there is a plastic interlaminar displacement angle in the support structure, which is represented by θ. The rotation of the connected beam relative to this displacement angle is represented by α:

$$\alpha = \frac{\alpha_A^s + \alpha_A^b + \alpha_B^s + \alpha_B^b}{2}, \tag{6}$$

where α_A^s represents the shear deformation angle of the A end of the connecting beam, α_B^s represents the shear deformation angle of the B end of the connecting beam, α_A^b represents the bending deformation angle of the A end of the connecting beam, and α_B^b represents the bending deformation angle of the B end of the connecting beam.

According to the ideal elastic-plastic theory [14], when the support is in the ultimate state, there are equal bending moments at the two endpoints of the shear yield type connected beam, that is, $M_A = M_B$, which represent the bending moments at A end and B end of the connected beam, respectively, and the bending moments are equal to $V_u e/2$. Thus, the virtual work of internal shear force can be calculated as follows:

$$W_{NL} = V_u \times e \times V, \tag{7}$$

where V_u represents the ultimate bearing capacity of the coupling beam and e and V represent the length of the coupling beam and the shearing force in the bracket, respectively. When the limit state is set, the bracket will be lifted up, and the disc spring in the direct structure will be compressed to produce the ultimate deformation. Meanwhile, the component accumulates a part of elastic potential energy. The total virtual work of internal force can be calculated using

$$W_N = V_u \times a + M_{cp} + k \times S_1 \times \theta, \tag{8}$$

where a represents the virtual work of internal force, M_{cp} represents the virtual work of internal force of the plastic hinge at the bottom of the bracket side column, S_1 and k represent the stiffness and ultimate compression limit of the disc spring, respectively, and θ represents the plastic bending bearing capacity.

3.3. 3D Model of Complex Steel Structure for Mine Protection. The virtual work caused by external force consists of two parts, namely, the virtual work caused by vertical load and the virtual work caused by horizontal external force. Generally, the position of the support column only has minimal axial pressure, which is not considered. However, the virtual work caused by concentrated load at the top of the connected column should be taken into account. The virtual work is expressed by P, and the virtual work caused by external force is expressed by

$$W_W = H \times \theta - P \times a \times \theta, \tag{9}$$

where H represents the distance between the beam on the bracket and the bracket foot. Referring to the virtual work principle, W_N is equal to W_W [15]. The ultimate shear strength of the connecting beam in the bracket meets the relation $V_u = 1.5V$. By substituting this relationship into the derivation results, the horizontal ultimate strength of the bracket can be obtained:

$$F = \frac{1.5V_u + P \times a + M_{cp} + k \times S_1 \times a}{H}. \tag{10}$$

According to the virtual work principle, the horizontal load in the ultimate state can be obtained:

$$\sum_{i=1}^{n} F_i H_i = \sum_{i=1}^{n} V_{ui} + P + M_{cp}, \tag{11}$$

where V_{ui} represents the ultimate shear strength and F_i and H_i represent the distance between the horizontal load of the i layer and the bottom of the support beam, respectively. The prototype structure of the model is the pipe support of polygon mine protection complex steel structure [16, 17]. The model is designed by SAP2000 finite element software with reference to the relevant steel structure codes and regulations. The three-dimensional model of the complex steel structure is shown in Figure 3.

In Figure 3, 1 represents the roof truss, 2 represents the bracket, 3 represents the dazzling transverse support, 4

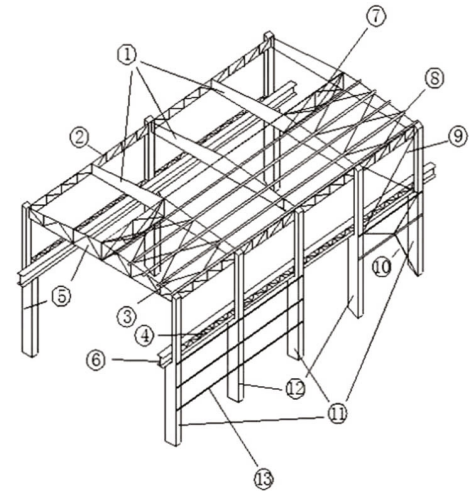

Figure 3: Three-dimensional model drawing of complex steel structure.

Table 2: Experimental parameter settings.

Name	Parameter
Reversing valve	Maximum traffic of 450 L/min
Push jack	Lifting capacity of 50 tons Lifting speed of 2.0 m/min
Steel	Q235B steel
Web bar	$\Phi 89 \times 5$ seamless steel tube
Chord	$\Phi 168 \times 9$ seamless steel tube
Supporting apex	$I350 \times 300 \times 14 \times 18$ seamless steel tube

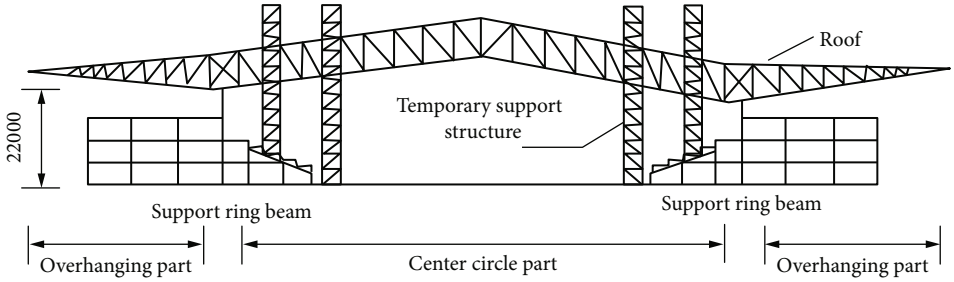

Figure 4: Long-span steel structure roof model.

Table 3: Initial values of vibration and set of control objectives.

Number of survey point	Vibrational serial number	Initial value		Control target value	
		Vibration frequency (Hz)	Amplitude of vibration	Vibration frequency (Hz)	Amplitude of vibration
1	1	109	1.563	65	1.024
	2	112	1.565	67	1.012
2	1	89	1.627	62	1.123
	2	87	1.315	61	0.984
3	1	101	1.628	66	1.131
	2	91	1.731	64	1.145

Table 4: Experimental results of vibration control for steel structures.

Number of survey point	Serial number	Method in reference [3]		Method in reference [4]		Design method	
		Vibration frequency (Hz)	Amplitude of vibration	Vibration frequency (Hz)	Amplitude of vibration	Vibration frequency (Hz)	Amplitude of vibration
1	1	66.1	1.031	65.3	1.028	65.1	1.025
	2	67.8	1.025	67.2	1.018	67.1	1.015
2	1	62.9	1.134	62.1	1.129	62.0	1.124
	2	62.1	0.998	61.4	0.992	61.0	0.987
3	1	67.1	1.140	66.5	1.137	66.3	1.134
	2	64.7	1.152	64.3	1.149	64.2	1.146

Table 5: Comparison of results before and after optimization.

Name	Before optimization	After optimization
Maximum displacement	0.4 mm	0.2 mm
Maximum stress	335 MPa	215 MPa
Mass	5.5 kg	3.1 kg
Are design requirements met	No	Yes

Table 6: Stress results.

Indicator	Maximum primary stress	Maximum 2nd stress
Maximum (kPa)	40215.7	66077.6
Allowed values (kPa)	92527.5	260568.8
Evaluation	Up to standard	Up to standard

represents the braking truss, 5 represents the transverse plane frame, 6 represents the crane beam, 7 represents roof trusses, 8 represents purlins, 9 and 10 represent intercolumn support, 11 represents frame columns, 12 represents intermediate columns, and 13 represents wall beams [18, 19]. The whole length of the truss is 44300 mm, the height is 8600 mm, and the support material is Q235 steel. One layer of the support structure is selected as the finite element analysis model, the section is 40 mm* 25 mm* 14 mm, and the 3D modeling of complex steel structure for mine protection based on BIM technology is completed.

4. Experimental Analysis

Experiments are conducted to verify the feasibility of 3D modeling of complex steel structure for mine protection based on BIM technology. The experimental parameters are shown in Table 2.

Table 7: Port thrust results.

Node	Working condition	Thrust (N)	Thrust torque (N·m)	Evaluation
101	Cold state	18563	18006	Equipment manufacturer's qualification
	Thermal state	19725	93682	Equipment manufacturer's qualification
102	Cold state	19696	20540	Equipment manufacturer's qualification
	Thermal state	28247	143864	Equipment manufacturer's qualification
103	Cold state	16346	30847	Equipment manufacturer's qualification
	Thermal state	98321	140788	Equipment manufacturer's qualification
104	Cold state	18706	19091	Equipment manufacturer's qualification
	Thermal state	131451	145641	Equipment manufacturer's qualification

The process of 3D modeling of complex steel structure for mine protection is as follows:

Step 1: determine the appropriate mine protective undercarriage program and demolition support program

Step 2: use the finite element analysis software to establish the finite element model of mine protective structure, temporary support, and jack, and then, apply the load according to the mine protective undercarriage scheme and the dismantling scheme

(1) Select grid type and define analysis type

(2) Add material properties

(3) Impose restraints

(4) Definition of load

(5) Grid generation

Step 3: use unit birth and death technology to process the unit in the model, namely, killing first and activating later. The main structure and temporary support of mine protection are returned to zero after being killed first, and then being activated, the dismantled support is returned to its original state

Step 4: the first step is to analyze the support structure. According to the result of step 1, the jack is pushed down one by one, and its supporting force is unloaded

Step 5: analyze the second step, continue to push down jack, and clear mine protective roof structure and jack top contact mode on the balance of the whole structural system

Step 6: repeat step 5 until all the jacks are separated from the main structure and then dismantle the supports. The mine protection structure and temporary support of the stress state and deformation changes can be obtained

The model of complex steel structure roof of mine protection is shown in Figure 4.

The safety standard of steel structure vibration is set synthetically, and the initial vibration and control target data are determined, as shown in Table 3.

Through three different control algorithms for complex steel structure vibration control, the vibration control results can be obtained, as shown in Table 4.

By comparing the data in Table 3 with the vibration control target data, the vibration control error under different vibration control algorithms can be obtained. The average control error of the method in reference [3], the method in reference [4], and the designed method is 0.48, 0.15, and 0.06, respectively. Therefore, the 3D modeling of complex steel structure for mine protection based on BIM technology has higher control accuracy.

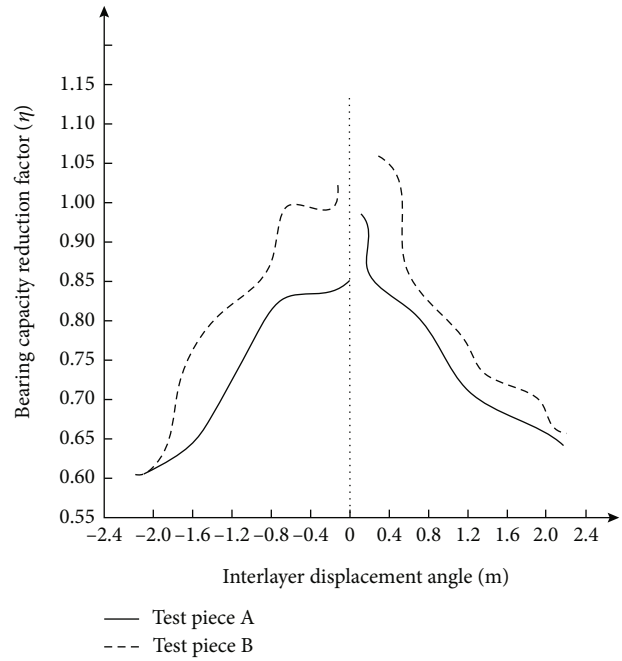

Figure 5: Strength degradation curve.

The analysis results before and after optimization of complex steel structure supports for mine protection are shown in Table 5.

It can be seen from Table 2 that the maximum displacement, maximum stress, and mass of the optimized complex steel support are reduced by half, which are 120 MPa and 2.4 kg, respectively, meeting the design requirements. The static load is calculated based on the structural parameters, operating conditions, and endpoint displacement of the pipeline, and the output results are shown in Tables 6 and 7.

According to Tables 6 and 7, the maximum stress on the complex steel structure 1 of the mine protection is less than the allowable stress, and it can be considered that the rated thrust and torque of the pipeline under cold and hot conditions can meet the requirements of the equipment manufacturer. The complex protection of the mine steel structure selected in this study is more reasonable and has a certain role in dispersing the stress.

Under the same displacement amplitude, the ratio of the last cyclic peak point load to the first cyclic peak point is represented by the bearing capacity reduction coefficient η, and the strength degradation is represented by the bearing capacity reduction coefficient. Figure 5 shows the strength degradation curve of specimens A and B of complex steel structure for mine protection.

It can be seen from Figure 5 that the degradation of bearing capacity of complex steel structure sample A is slightly higher than that of complex steel structure sample B, but the difference between them is not great. In the later period of loading, the degradation degree of sample A of complex steel structure is significantly higher than that of sample B. This is because the complex steel structure specimen B is protected by stiffener, which can delay the strength degradation of the specimen. Under the same loading capacity, the reduction coefficient of the bearing capacity is inversely proportional to the interstory displacement angle, and the degradation of the bearing capacity increases with the increase of the loading capacity.

5. Conclusion and Prospect

5.1. Conclusion. A friction slider can dissipate most of the vibration energy in the directional contact with the sliding surface, cope with the huge resistance from the lower structure, and provide gravity support for the upper structure in the movement of other parts of the device (such as rollers and rolling balls). Through the design and application of 3D modeling of complex steel structures for mine protection based on BIM technology, accurate reference data are provided for vibration isolation and seismic design of complex structures for mine protection, which is helpful to extend the service life of concrete buildings. The simulation results based on BIM model show that, with the increase of bearing capacity, the performance degradation of reinforced ribbed box plate steel structure is significantly lower than that of unreinforced ribbed box plate steel structure, and the reduction of strength and stiffness of sample A is more significant than that of sample B.

5.2. Prospect

(1) The BIM field lacks uniform and professional industry standards. It is hoped that the relevant staff responsible for preparing construction standards in China can formulate a set of practical standard documents as soon as possible, so as to promote the development of BIM technology in China and facilitate the application of such technology in the mining industry

(2) Most mining enterprises have a certain understanding of BIM technology, but the actual application degree of BIM technology remains unclear, which is worth further research. This research is of great importance for the improvement of production safety in the industry

(3) Researches on the life cycle of the project with the application of BIM technology are mainly concentrated on the design and construction stages, but the operation, maintenance, and management stages are relatively ignored. The BIM application should be promoted through the education and training of users, so as to maximize the rational use of resources and intelligent engineering construction

Data Availability

The datasets used and/or analyzed during the current study are available from the author on reasonable request.

Conflicts of Interest

The authors declare no conflicts of interest regarding this article.

Acknowledgments

The research is financially supported by the Zhejiang Provincial Construction Scientific Research Project: Research on the Application of BIM Technology in the Design of Complex Steel Structure (No. 2020K203).

References

[1] D. Jrg, "Radon exposures of miners at small underground construction sites in old mining: recommendations to improve radiation protection measures by the Saxon radiation protection authority," *Health Physics*, vol. 118, no. 1, pp. 96–105, 2020.

[2] Y. N. Wang, "Solidification structure, non-metallic inclusions and hot ductility of continuously cast high manganese TWIP steel slab," *ISIJ International*, vol. 59, no. 5, pp. 872–879, 2019.

[3] H. Ye, T. Wang, C. Wu, Z. Duan, and C. Liu, "A comparative analysis of driving force models for fatigue crack propagation of CFRP-reinforced steel structure," *International Journal of Fatigue*, vol. 130, no. 1, article 105266, 2020.

[4] Y. Xiang, Y. Koetaka, and N. Okuda, "Single-story steel structure with LVEM-isolated floor: elastic seismic performance and design response spectrum," *Engineering Structures*, vol. 196, no. 10, article 109314, 2019.

[5] P. Karan, S. S. Das, R. Mukherjee, J. Chakraborty, and S. Chakraborty, "Flow and deformation characteristics of a flexible microfluidic channel with axial gradients in wall elasticity," *Soft Matter*, vol. 16, no. 24, pp. 5777–5786, 2020.

[6] J. S. Kwan, E. H. Y. Sze, and C. Lam, "Finite element analysis for rockfall and debris flow mitigation works," *Canadian Geotechnical Journal*, vol. 56, no. 9, pp. 1225–1250, 2019.

[7] K. Zhang, M. Ainslie, M. Calvi, S. Hellmann, R. Kinjo, and T. Schmidt, "Fast and efficient critical state modelling of field-cooled bulk high-temperature superconductors using a backward computation method," *Superconductor Science and Technology*, vol. 33, no. 11, article 114007, 2020.

[8] X. Lei, P. Chen, H. Hou, S. Liu, and P. Liu, "Longitudinal vibration wave in the composite elastic metamaterials containing Bragg structure and local resonator," *International Journal of Modern Physics B*, vol. 34, no. 26, article 2050232, 2020.

[9] R. Andreani, N. S. Fazzio, M. L. Schuverdt, and L. D. Secchin, "A sequential optimality condition related to the quasi-normality constraint qualification and its algorithmic consequences," *SIAM Journal on Optimization*, vol. 29, no. 1, pp. 743–766, 2019.

[10] K. Li and Y. Ou, "Global wellposedness of vacuum free boundary problem of isentropic compressible magnetohydrodynamic equations with axisymmetry," *Discrete & Continuous Dynamical Systems - B*, vol. 27, no. 1, p. 487, 2022.

[11] A. Mantziris, A. Pastore, I. Vidaña, D. P. Watts, M. Bashkanov, and A. M. Romero, "Neutron star matter equation of state including d*-hexaquark degrees of freedom," *Astronomy and Astrophysics*, vol. 638, no. 16, article A40, 2020.

[12] C. P. Wu, Y. J. Chen, and Y. M. Wang, "Three-dimensional asymptotic nonlocal elasticity theory for the free vibration analysis of embedded single-walled carbon nanotubes," *Computers & Mathematics with Applications*, vol. 80, no. 1, pp. 161–182, 2020.

[13] S. R. Li and H. K. Ma, "Analysis of free vibration of functionally graded material micro-plates with thermoelastic damping," *Archive of Applied Mechanics*, vol. 90, no. 6, pp. 1285–1304, 2020.

[14] M. Barral, G. Chatzigeorgiou, F. Meraghni, and R. Léon, "Homogenization using modified Mori-Tanaka and TFA framework for elastoplastic- viscoelastic-viscoplastic composites: theory and numerical validation," *International Journal of Plasticity*, vol. 127, article 102632, 2020.

[15] K. D. Chen, J. P. Liu, J. Q. Chen et al., "Equivalence of Lagrange's equations for non-material volume and the principle of virtual work in ALE formulation," *Acta Mechanica*, vol. 231, no. 3, pp. 1141–1157, 2020.

[16] P. V. Badiger, V. H. Desai, M. R. Ramesh, B. K. Prajwala, and K. Raveendra, "Effect of cutting parameters on tool wear, cutting force and surface roughness in machining of MDN431 alloy using Al and Fe coated tools," *Materials Research Express*, vol. 6, no. 1, article 016401, 2019.

[17] P. V. Badiger, V. H. Desai, M. R. Ramesh, S. Joladarashi, and H. Gourkar, "Tribological behaviour of monolayer and multilayer Ti-based thin solid films deposited on alloy steel," *Materials Research Express*, vol. 6, no. 2, article 026419, 2018.

[18] P. V. Badiger, V. Desai, M. R. Ramesh, B. K. Prajwala, and K. Raveendra, "Cutting forces, surface roughness and tool wear quality assessment using ANN and PSO approach during machining of MDN431 with TiN/AlN-coated cutting tool," *Arabian Journal for Science and Engineering*, vol. 44, no. 9, pp. 7465–7477, 2019.

[19] P. V. Badiger, V. Desai, and M. R. Ramesh, "Development and characterization of Ti/TiC/TiN coatings by cathodic arc evaporation technique," *Transactions of the Indian Institute of Metals*, vol. 70, no. 9, pp. 2459–2464, 2017.